Structure, Bonding, and Paramagnetism in the Manganese(II) Tris-Allyl Anions $[Mn\{\eta^x\text{-}(C_3H_3R_2)_3\}]^-$ (R = H, $SiMe_3$; x = 1 or 3): Insight from Theory

Richard A. Layfield,*,‡ Michael Bühl,*,# and Jeremy M. Rawson‡

Department of Chemistry, University of Cambridge, Lensfield Road, Cambridge, CB2 1EW, United Kingdom, and Max-Planck-Institut für Kohlenforschung, Kaiser-Wilhelm-Platz 1, D-45470 Mülheim an der Ruhr, Germany

Received April 4, 2006

Geometry optimizations of the $[Mn\{\eta^x\text{-}(Me_3Si)_2C_3H_3\}_3]^-$ anion and its parent anion $[Mn(\eta^x\text{-}C_3H_5)_3]^-$ in the high-spin or $S = 5/2$ state at the BP86/AE1 level of theory yielded the mixed hapticity structures $[Mn\{\eta^3\text{-}(Me_3Si)_2C_3H_3\}\{\eta^1\text{-}(Me_3Si)_2C_3H_3)_2\}]^-$ and $[Mn(\eta^3\text{-}C_3H_5)(\eta^1\text{-}C_3H_5)_2]^-$ (**1-HS** and **2-HS**, respectively). These calculations revealed that the silyl substituents in **1-HS** have very little influence on the hapticities of the ligands and the asymmetric bonding of the η^3-bonded ligand, suggesting that these structural features are intrinsic to the complex. Natural population analyses and calculations of Wiberg bond indices for **1-HS** indicate predominantly ionic bonding between manganese and the η^3-bonded ligands, while there is increased covalent character in the bonds to the η^1-bonded ligands. Investigations of the related intermediate-spin forms of these complexes for which $S = 3/2$ afford structures of composition $[Mn\{\eta^3\text{-}(Me_3Si)_2C_3H_3\}_2\{\eta^1\text{-}(Me_3Si)_2C_3H_3)\ \}]^-$ (**1-IS**) and $[Mn(\eta^3\text{-}C_3H_5)_2(\eta^1\text{-}C_3H_5)]^-$ (**2-IS**), in which one of the allyl ligands has slipped from an η^1- to η^3-bonding mode with a concomitant decrease in the manganese−carbon distances, and which again reveals essentially no dependency of hapticity upon the spatial requirements of the silyl substituents. The relative energies of **1-HS**, **1-IS**, and the low-spin state **1-LS** (for which $S = 1/2$) at both the BP86/AE1 and B3LYP/AE1 levels of theory revealed **1-HS** and **1-LS** to be the most and least stable forms of **1**, respectively, with the energy of **1-LS** being prohibitively high at each level of theory. A reinvestigation of the experimental magnetic susceptibility of the ion-separated species $[Li(thf)_4][Mn\{\eta^3\text{-}(Me_3Si)_2C_3H_3\}\{\eta^1\text{-}(Me_3Si)_2C_3H_3)_2\}]$, $[Li(thf)_4][\mathbf{1}]$, yielded a Curie constant that indicated the presence of an $S = 3/2$ spin state for the Mn(II) ion.

Introduction

Since the discovery of manganocene, Cp_2Mn, in 1954, the organometallic chemistry of manganese in the oxidation state +2 has been dominated by the ubiquitous cyclopentadienide ligands.[1,2] The reluctance of manganese(II) to form stable complexes with neutral π-acidic ligands such as carbon monoxide and olefins has been rationalized in terms of the preference of this metal ion to engage in ionic bonding. A similar paucity of complexes in which manganese(II) is π-bonded to other, formally anionic ligands is, however, less readily explained, and despite the many similarities between the cyclopentadienide and allyl (or "propenide") ligands, the allyl chemistry of manganese(II) has evolved at a much slower pace. Indeed, an early review article even described the understanding of manganese(II) allyl chemistry as "obscure".[3] The situation became somewhat less obscure when the first structurally authenticated manganese(II) allyl complex, $[Mn\{\eta^3\text{-}(Me_3Si)_2C_3H_3\}\{\eta^1\text{-}(Me_3Si)_2C_3H_3\}_2]\text{-}[Li(thf)_4]$, $[\mathbf{1}][Li(thf)_4]$, was reported.[4]

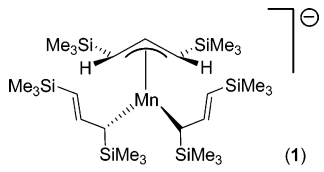

(1)

Due to the radially contracted nature of the valence 3d orbitals within complexes of manganese(II), the metal−ligand bonds in the pseudo-tetrahedral complex **1** were assumed to be predominantly ionic in nature; hence the mixed hapticity of the allyl ligands was particularly noteworthy since ionic metal allyl complexes typically exhibit a preference for either η^1-bonding, such as in the case of magnesium,[5] or η^3-bonding, such as in the case of the alkali and lanthanide metals,[6,7] but the occurrence of both bonding modes simultaneously is rare. Asymmetry in the Mn−$[\eta^3\text{-}(Me_3Si)_2C_3H_3]$ connectivity of **1** was revealed through the terminal Mn−C distances of 2.470(4) and 2.398-

* To whom correspondence should be addressed. E-mail: ral34@cam.ac.uk; buehl@mpi-muelheim.mpg.de.

‡ University of Cambridge.

Max-Planck-Institut für Kohlenforschung.

(1) Wilkinson, G.; Cotton, F. A. *Chem. Ind.* **1954**, *11*, 307. (b) Wilkinson, G.; Cotton, F. A.; Birmingham, J. M. *J. Inorg. Nucl. Chem.* **1956**, *2*, 95.

(2) Sitzmann, H. *Coord. Chem. Rev.* **2001**, *214*, 287.

(3) Wilke, G.; Bogdanovic, B.; Hardt, P.; Heimbach, P.; Keim, W.; Kröner, M.; Oberkirch, W.; Tanaka, K.; Steinrücke, E.; Walter, D.; Zimmermann, H. *Angew. Chem., Int. Ed.* **1966**, *5*, 151.

(4) Layfield, R. A.; Humphrey, S. M. *Angew. Chem., Int. Ed.* **2004**, *43*, 3067.

(5) Marsch, M.; Harms, K.; Massa, W.; Boche, G. *Angew. Chem., Int. Ed.* **1987**, *26*, 696. (b) Bailey, P. J.; Liddle, S. T.; Morrison, C. A.; Parsons, S. *Angew. Chem., Int. Ed.* **2001**, *40*, 4463.

10.1021/om060295a CCC: $33.50 © 2006 American Chemical Society
Publication on Web 06/22/2006

(4) Å, with the central Mn−C distance being 2.348(3) Å, a structural feature that has also been observed in the structures of some allyl complexes of the alkali and transition metals.[3,6] The Mn−C distances to the η^1-bonded ligands in **1** were essentially identical at 2.184(4) and 2.187(4) Å. The presumed importance of kinetic factors in the stability of **1**, by virtue of the voluminous trimethylsilyl substituents, led to the assertion that the mixed η^3:η^1:η^1 hapticities and the asymmetry of the Mn−[η^3-(Me_3Si)$_2C_3H_3$] bond were probably due to the steric requirements of the ligand periphery, although involvement of crystal-packing effects could not be discounted since they are known to be able to influence ligand hapticities in polar/ionic organometallics.[8] Temperature-dependent magnetic properties bestow **1** with additional interest: at 5 K the effective magnetic moment, μ_{eff}, is equal to 2.92 μ_B and increased steadily with temperature to reach 4.03 μ_B at 300 K. This observation was attributed to a gradual population of the high-spin $S = 5/2$ state of Mn(II) at the expense of the low-spin $S = 1/2$ state and is qualitatively similar to the magnetic properties of the previously reported [(η^2-Cp)$_3$Mn]$^-$ anion and several substituted derivatives of manganocene.[2,9] In addition to the interest in the fundamental properties of tris-(organo)manganate anions such as **1**, [Cp_3Mn]$^-$, and the σ-bonded complex [Mes_3Mn]$^-$ (Mes = mesityl),[10] compounds of this type are increasing in popularity as alternative carbanion sources in organic and organometallic synthesis.[11]

Despite the quantitative structural information available for the anion **1**, a number of fundamental questions about the allyl−manganese(II) connectivity remain to be addressed. To develop an understanding of the nature of the manganese−allyl bonding in complex **1** and the factors upon which its molecular structure and magnetic properties depend, we have undertaken a density functional theory (DFT) investigation into the [Mn{η^x-(Me_3Si)$_2C_3H_3$)$_3$}]$^-$ anion and its unsubstituted "parent" anion [Mn{η^x-C_3H_5)$_3$}]$^-$ (**2**) and on the basis of the results of these calculations have undertaken a more detailed examination of the magnetic properties of the previously reported complex [**1**]-[Li(thf)$_4$].

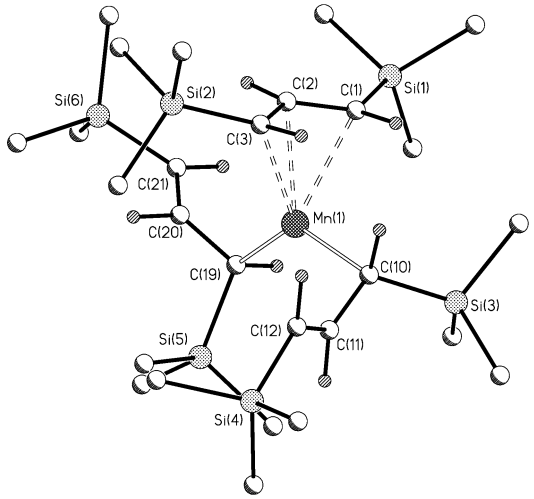

Figure 1. Structure of **1-HS** calculated at the BP86/AE1 level of theory. For clarity, only the allyl hydrogens are shown.

Computational Details

Geometries were fully optimized at the BP86/AE1 level, i.e., employing the exchange and correlation functionals of Becke[12] and Perdew,[13] respectively, together with a fine integration grid (75 radial shells with 302 angular points per shell), the augmented Wachters' basis[14] on Mn (8s7p4d), and 6-31G* basis[15] on all other elements. This and comparable DFT levels have proven quite successful for transition metal compounds and are well suited for the description of structures, energies, barriers, and other properties.[16] The unrestricted Kohn−Sham formalism was employed throughout. Spin contamination was small for sextet and quartet states, with $\langle \hat{S}^2 \rangle$ values up to ca. 8.78 and 3.87, respectively (instead of the expected 8.75 and 3.75), and was significantly larger for doublet states (up to 1.65 instead of the expected 0.75). Single-point energies were evaluated for the BP86/AE1 geometries at the B3LYP/AE1 level, that is, using the functionals according to Becke (hybrid)[17] and Lee, Yang, and Parr.[18] All computations employed the Gaussian 03 program package.[19]

Results and Discussion

Initial geometry optimization of the [Mn{η^x-(Me_3Si)$_2C_3H_3$)$_3$}]$^-$ anion in the high-spin, $S = 5/2$ state (**1-HS**) was started from the X-ray-derived coordinates of the ion in the solid.[4] No qualitative changes of this structure (such as hapticities of the ligands) occurred during minimization, and the final, optimized structural parameters are in good agreement with experiment. An interesting result is the enhanced asymmetry in the bonding of the [η^3-(Me_3Si)$_2C_3H_3$)$_3$] ligand to Mn(1) in **1-HS**. The Mn(1)−C(1) and Mn(1)−C(3) distances were calculated to be 2.488 and 2.365 Å, respectively, with the difference of 0.123 Å comparing to a somewhat smaller analogous difference of 0.072 Å found in the experimental structure of **1** (Figure 1 and Table 1).

(6) Fernández-Galán, R.; Hitchcock, P. B.; Lappert, M. F.; Antiñolo, A.; Rodríguez, A. *J. Chem. Soc., Dalton Trans.* **2000**, 1743. (b) Boche, G.; Fraenkel, G.; Cabral, J.; Harms, K.; van Eikemma Hommes, N. J. R.; Lohrenz, J.; von Ragué Schleyer, P. *J. Am. Chem. Soc.* **1992**, *114*, 1562. (c) van Eikemma Hommes, N. J. R.; Bühl, M.; von Ragué Schleyer, P. *J. Organomet. Chem.* **1991**, *409*, 307. (d) Fraenkel, G.; Chow, A.; Winchester, W. R. *J. Am. Chem. Soc.* **1990**, *112*, 1382. (e) Schümann, U.; Weiss, E.; Dietrich, H.; Mahdi, W. *J. Organomet. Chem.* **1987**, *322*, 299. (f) Boche, G.; Etzrodt, H.; Marsch, M.; Massa, W.; Baum, G.; Dietrich, H.; Mahdi, W. *Angew. Chem., Int. Ed.* **1986**, *25*, 104.

(7) Sánchez-Barba, L. F.; Hughes, D. L.; Humphrey, S. M.; Bochmann, M. *Organometallics* **2005**, *24*, 5329. (b) Woodman, T. J.; Schormann, M.; Hughes, D. L.; Bochmann, M. *Organometallics* **2004**, *23*, 2972. (c) Woodman, T. J.; Schormann, M.; Hughes, D. L.; Bochmann, M. *Organometallics* **2003**, *22*, 3028. (d) Woodman, T. J.; Schormann, M.; Bochmann, M. *Organometallics* **2003**, *22*, 2938.

(8) Morrison, C. A.; Layfield, R. A.; Wright, D. S. *J. Am. Chem. Soc.* **2002**, *124*, 6775.

(9) Bond, A. D.; Layfield, R. A.; MacAllister J. A.; McPartlin, M.; Rawson, J. M.; Wright, D. S. *J. Chem. Soc., Chem. Commun.* **2001**, 1956. (b) Soria Alvarez, C.; Bashall, A.; McInnes, E. J. L.; Layfield, R. A.; Mole, R. A.; McPartlin, M.; Rawson, J. M.; Wood, P. T.; Wright, D. S. *Chem. Eur. J.* **2006**, *12*, 3053. (c) Kheradmandan, S.; Schmalle, H. W.; Jacobsen, H.; Blacque, O.; Fox, T.; Berke, H.; Gross, M.; Decurtins, S. *Chem. Eur. J.* **2002**, *8*, 2526.

(10) Bartlett, R. A.; Olmstead, M. M.; Power, P. P.; Shoner, S. C. *Organometallics* **1988**, *24*, 1801.

(11) Oshima, K. J. *Organomet. Chem.* **1999**, *575*, 1. (b) Ley, S. V.; Koukolvsky, C. In *Comprehensive Organic Functional Group Transformations*, 1st ed.; Katritzky, A. R., Meth-Cohn, O., Rees, C. W., Eds.; Elsevier Science Ltd.: 1995; Vol. 2, p 538.

(12) Becke, A. D. *Phys. Rev. A* **1988**, *38*, 3098.

(13) Perdew, J. P. *Phys. Rev. B* **1986**, *33*, 8822. (b) Perdew, J. P. *Phys. Rev. B* **1986**, *34*, 7406.

(14) Wachters, A. J. H. *J. Chem. Phys.* **1970**, *52*, 1033. (b) Hay, P. J. *J. Chem. Phys.* **1977**, *66*, 4377.

(15) Hehre, W. J.; Ditchfield, R.; Pople, J. A. *J. Chem. Phys.* **1972**, *56*, 2257. (b) Hariharan, P. C.; Pople, J. A. *Theor. Chim. Acta* **1973**, *28*, 213.

(16) See for instance: Koch, W.; Holthausen, M. C. *A Chemist's Guide to Density Functional Theory*; Wiley-VCH: Weinheim, 2000; and the extensive bibliography therein.

(17) Becke, A. D. *J. Chem. Phys.* **1993**, *98*, 5648.

(18) Lee, C.; Yang, W.; Parr, R. G. *Phys. Rev. B* **1988**, *37*, 785.

(19) *Gaussian 03*; Gaussian, Inc.: Pittsburgh, PA, 2003. See Supporting Information for full citation.

Table 1. Selected Bond Lengths (Å, BP86/AE1 level) for 1-HS, 2-HS, 1-IS, and 2-IS

	1[a]	1-HS	2-HS-A	2-HS-B	2-HS-C	2-HS-D	2-HS-E	1-IS	2-IS
Mn(1)−C(1)	2.470(4)	2.488	2.513	2.292	2.473	2.513	2.161	2.312	2.222
Mn(1)−C(2)	2.348(3)	2.321	2.288	2.286	2.297	2.331		2.091	2.068
Mn(1)−C(3)	2.398(4)	2.365	2.282	2.501	2.338	2.531		2.219	2.153
Mn(1)−C(10)	2.184(4)	2.184	2.151	2.148	2.146	2.513	2.161	2.226	2.147
Mn(1)−C(11)						2.331		2.100	2.067
Mn(12)−C(12)						2.531		2.328	2.239
Mn(1)−C(19)	2.187(4)	2.184	2.169	2.167	2.160	2.513	2.161	2.192	2.159
Mn(1)−C(20)						2.331			
Mn(1)−C(21)						2.531			

[a] Experimental values taken from ref 4.

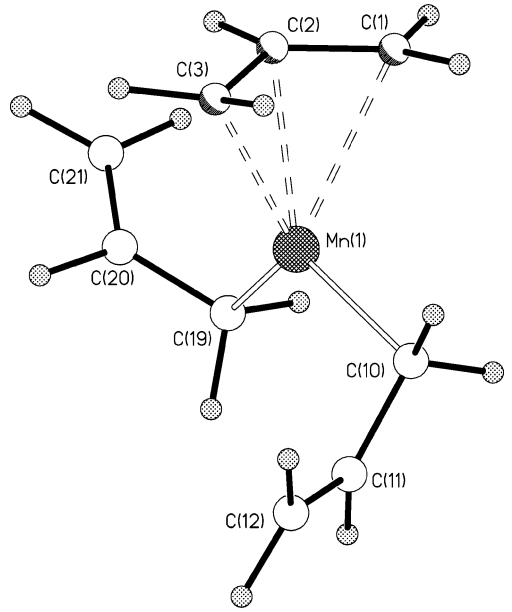

Figure 2. Structure of **2-HS-A** calculated at the BP86/AE1 level of theory.

This leads to the conclusion that the asymmetry in the bonding of the $[\eta^3\text{-}(Me_3Si)_2C_3H_3]$ ligand to manganese is intrinsic to the complex and is not attributable to the effects of packing in the crystal, and raises the question of the influence of the trimethylsilyl substituents on hapticity. To address this question, we performed optimizations for the parent high-spin complex $[Mn(C_3H_5)_3]^-$ (**2-HS**). An initial minimization started from the BP86 structure of **1-HS**, replacing the trimethylsilyl substituents with hydrogen atoms. In the resulting minimum no changes in hapticity from **1-HS** were found (Figure 2 and Table 1). However, the Mn(1)−C(10) and Mn(1)−C(19) distances to the η^1-bonded ligands in **2-HS-A** were both calculated to shorten slightly by 0.033 and 0.018 Å, respectively, which is probably due to the absence of the Me_3Si substituents. More intriguing is the impact of removing the substituents upon the η^3-bonded ligand since Mn(1)−C(1) was calculated to lengthen by 0.043 Å to 2.513 Å, but both Mn(1)−C(2) and Mn(1)−C(3) were shortened by 0.060 and 0.116 Å to 2.288 and 2.828 Å, respectively. Overall, therefore, in the seemingly sterically less crowded environment of $[Mn(\eta^3\text{-}C_3H_5)(\eta^1\text{-}C_3H_5)_2]^-$ an *increase* in the asymmetric bonding mode of the η^3-allyl ligand occurs relative to that in complexes **1** and **1-HS**. In the absence of any obvious electronic influences the enhanced asymmetry in the $[\eta^3\text{-}C_3H_5]$-Mn(1) bond in **2-HS-A** most likely occurs as a result of subtle changes in the nonbonded interactions between the η^3- and η^1-bonded ligands that stem from a shortening of the Mn(1)−C(4) and Mn(1)−C(7) bonds, which is also reflected in an increase in the C(1)−Mn(1)−C(4) bond angles from 101.6° in **1-HS** to 107.2° in **2-HS-A**.

Subsequently, we searched specifically for other hapticities and attempted to locate isomers of this parent complex with η^3:η^3:η^3 and η^3:η^3:η^1 coordination modes. Two new minima were thus found, **2-HS-B** and **2-HS-C**, but these also have optimized to structures with η^3:η^1:η^1 ligand hapticities. Since these minima differ from **2-HS-A** only in the precise conformations of the η^1-C_3H_5 ligands (see Supporting Information), it is not surprising that these three conformations are very similar in energy, with their relative energies calculated to be 0, −0.2, and 0.5 kcal mol^{-1} for **2-HS-A**, **2-HS-B**, and **2-HS-C**, respectively, at the BP86/AE1 level of theory. Other ligand hapticities could only be enforced by imposing symmetry constraints. Stationary point **2-HS-D** is a C_{3h}-symmetric structure in which all three allyl ligands are η^3-bonded to Mn(1), generating a trigonal prismatic coordination environment. This conformation, however, is 19.4 kcal mol^{-1} higher in energy than **2-HS-A** and is a higher-order saddle point with four imaginary frequencies (Figure 3). Lowering the symmetry from C_{3h} to C_3 finally

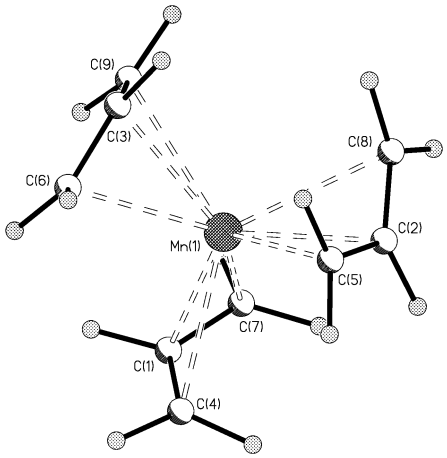

Figure 3. Structure of **2-HS-D** calculated at the BP86/AE1 level of theory.

resulted in stationary point **2-HS-E**, in which all the ligands adopt an η^1-bonded arrangement to afford a trigonal planar geometry at Mn(1). This structure (Figure 4) possesses two degenerate imaginary frequencies and is only 2.8 kcal mol^{-1} above **2-HS-B.** Following the intrinsic reaction coordinate[20] of one of these imaginary modes showed that **2-HS-E** describes an interconversion between two forms of **2-HS-B** in which η^3- and η^1-coordinated ligands are interchanged. Thus **2-HS** is predicted by theory to be a highly fluxional molecule.

In an attempt to develop a structure−property relationship between the geometric and magnetic properties of **1**, geometry optimizations on the intermediate-spin (**1-IS**) and low-spin (**1-LS**) states, for which $S = 3/2$ and 1/2, respectively, were

(20) Gonzalez, C.; Schlegel, H. B. *J. Chem. Phys.* **1989**, *90*, 2154. (b) Gonzalez, C.; Schlegel, H. B. *J. Phys. Chem.* **1990**, *94*, 5523.

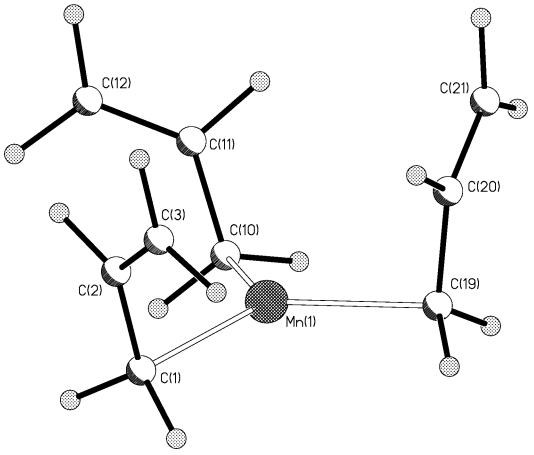

Figure 4. Structure of **2-HS-E** calculated at the BP86/AE1 level of theory.

Table 2. Relative Energies (kcal mol^{-1}) of 1-HS, 1-IS, and 1-LS Calculated at the BP86/AE1 and B3LYP/AE1 Levels of Theory

	BP86/AE1	B3LYP/AE1[a]
1-HS	0.0	0.0
1-IS	0.7	21.1
1-LS	16.4	42.9

[a] BP86/AE1 geometries employed.

undertaken. Initial optimizations of **1-LS** starting from the experimental coordinates of **1** were plagued by severe wave function convergence problems, which are probably related to the substantial spin contamination encountered in this case (see computational details). No such problems occurred for **1-IS**, which, interestingly, optimized to a structure with different hapticity (η^3:η^3:η^1, see below). Using this structure as starting point, **1-LS** could eventually be optimized (without further changes in hapticity). Relative energies for **1-HS**, **1-IS**, and **1-LS**, computed with two different density functionals, are collected in Table 2. Calculations of relative stabilities of different spin states in open-shell transition metal complexes are a notorious problem for DFT.[16,21] Consistent with previous experience in such cases, the results in Table 2 are strongly dependent on the particular functional used in the calculations.

However, despite the greatly differing values for the relative energies of the various spin states of **1**, it is beyond doubt that the energy of **1-LS** is prohibitively high at all levels of theory. The lowest-energy state for each functional is **1-HS**, which provides additional evidence that this structure is most probably that determined experimentally. At the BP86/AE1 level of theory the energy of **1-IS** is only 0.7 kcal mol^{-1} above that of **1-HS**, which is increased to 21.1 kcal mol^{-1} at B3LYP/AE1. This wide margin notwithstanding, it is possible that **1-HS** and **1-IS** could actually be quite close in energy, which would have implication for the temperature dependence of μ_{eff} (see below). If the latter is in fact due to variable population of isomers with different spin states, it is almost certain that it is **1-IS** with $S = 3/2$, and not **1-LS** with $S = 1/2$, that is in equilibrium with **1-HS**.

During optimization from a η^3:η^1:η^1 starting structure, **1-IS** was found to converge to a structure of composition [Mn{η^3-(Me_3Si)$_2C_3H_3$}$_2${η^1-(Me_3Si)$_2C_3H_3$)}]$^-$, i.e., one in which a ligand has undergone a change in hapticity from η^1 to η^3 (Figure 5).

In **1-IS** the manganese center is formally five-coordinate and resides within a distorted trigonal bipyramidal environment. The

(21) See for instance: Reiher, M. *Inorg. Chem.* **2002**, *41*, 6928.

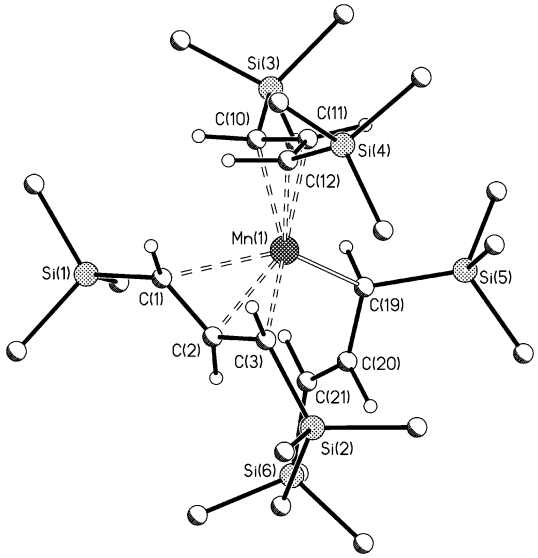

Figure 5. Structure of **1-IS** calculated at the BP86/AE1 level of theory. For clarity, only the allyl hydrogens are shown.

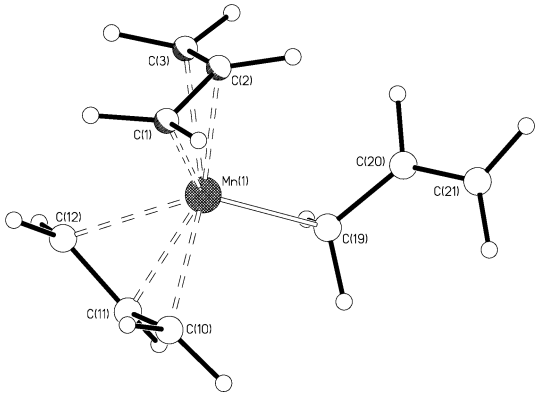

Figure 6. Structure of **2-IS** calculated at the BP86/AE1 level of theory.

Mn(1)−C(10), Mn(1)−C(11), and Mn(1)−C(12) distances were calculated to be 2.226, 2.100, and 2.328 Å, respectively, with the asymmetry in the bonding of this η^3-ligand to Mn(1) being similar to that seen in the experimental structure of **1** and the calculated structure **1-HS**. Significantly, the Mn(1)−C(1), Mn(1)−C(2), and Mn(1)−C(3) distances of 2.312, 2.091, and 2.219 Å, respectively, have *shortened* considerably relative to the analogous distances in **1-HS** rather than lengthened, as might be expected simply on steric grounds in order to accommodate the new η^3-bonded ligand. As shown in Figure 6, calculation of the parent intermediate-spin complex [Mn(C_3H_5)$_3$]$^-$ (**2-IS**) also results in an η^3:η^3:η^1 ligand arrangement and suggests that the hapticity change accompanying formation of the intermediate-spin state is intrinsic to the system and also that the Me_3Si substituents have little, if any, overall impact on this structural property. Comparison of the bond distances computed for **1-IS** and **1-HS** with those observed for **1** in the solid suggest that it is indeed the high-spin state of **1** that has been observed experimentally.[4]

The similar calculated energies of **1-HS** and **1-IS** at the BP86/AE1 level of theory prompted us to reinvestigate the experimental magnetic susceptibility data on [**1**][Li(thf)$_4$]. The conditions under which data were collected have been described previously.[4] Complex [**1**][Li(thf)$_4$] shows Curie−Weiss behavior from room temperature down to 100 K (Figure 7) ($C = 2.45$ emu·K·mol^{-1}, $\theta = -60$ K). The Curie constant, C, is substantially lower than that expected for spin-only $S = 5/2$

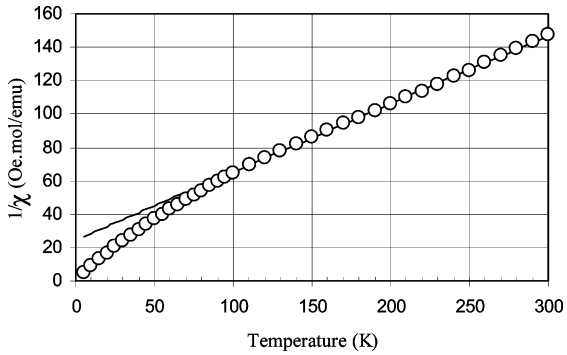

Figure 7. Magnetic behavior of **1**. Experimental data are presented as circles, and the solid line represents the high-temperature fit to Curie−Weiss behavior.

ions ($C = 4.377$ with $g = 2.0$) and substantially larger than the value anticipated for an $S = 1/2$ system ($C = 0.375$ with $g = 2.0$) and is in fact consistent with an intermediate-spin state with $S = 3/2$ ($C = 1.876$ with $g = 2.0$). An explanation of this observation on the basis of exchange interactions between nearest-neighbor Mn(II) ions can be discounted since the bulky nature of the ligands around these ions mitigate against any such effects and the large Weiss constant is likely to reflect single ion effects.

Whereas the majority of manganese(II) complexes display $S = 5/2$ spin states, observation of low-spin $S = 1/2$ states is comparatively rare, $[Mn(CN)_6]^{4-}$ being one notable exception.[22] The observation of an intermediate-spin or spin-admixed state for Mn(II) is also uncommon, and to the best of our knowledge [**1**][Li(thf)$_4$] is only the second reported example, the first having been found in the $[(\eta^2\text{-Cp}')_3Mn]^-$ anions (Cp′ = C_5H_5 or C_5H_4-Me).[9a,b] The $S = 3/2$ spin state for d^5 configurations is better documented in the chemistry of iron(III), where the sensitivity of the spin state to the ligand field is exemplified in a series of ferric porphyrin compounds where there is strong evidence for $S = 5/2$, 3/2, 1/2 and spin-admixed states.[23] It is worth noting at this juncture that the DFT studies indicate that the low-spin state is substantially higher in energy than both the $S = 3/2$ and $S = 5/2$ configurations, but also that the intermediate-spin state **1-IS** is within 1 kcal mol^{-1} of the ground state **1-HS** at the BP86/AE1 level of theory: when quartet and sextet states are so close in energy, they are likely to couple though spin−orbit coupling to generate a spin-admixed state.[24]

In an attempt to ascertain the reasons behind formation of the $S = 3/2$ state we undertook a more detailed examination of the Mn−C bonding in the anion **1**. In addition, given the lively debate that has taken place on the subject of the character of metal−carbon bonding in organometallic compounds of the main group elements, with the organolithiums in particular having been the subject of many theoretical studies,[25] we also address the fundamental question of the extent to which the Mn−C bonds in **1** are ionic or covalent. Atomic charges were calculated using natural population analysis (NPA).[26] In addition, we determined the Wiberg bond indices (WBIs),[27] a measure for the covalent contributions to a bonding interaction. The results are presented in Table 3.

Table 3. Natural Population Analyses and Wiberg Bond Indices for 1-HS and 1-IS Calculated at the BP86/AE1 Level of Theory

	NPA[a]			WBI	
	1-HS	**1-IS**		**1-HS**	**1-IS**
Mn(1)	+1.20	+0.79	Mn(1)−C(1)	0.12	0.28
C(1)	−0.98	−0.93	Mn(1)−C(2)	0.08	0.26
C(2)	−0.26	−0.29	Mn(1)−C(3)	0.16	0.38
C(3)	−1.02	−0.91	Mn(1)−C(11)	0.30	0.36
C(11)	−1.17	−0.92	Mn(1)−C(12)	0.03	0.27
C(12)	−0.19	−0.28	Mn(1)−C(13)	0.02	0.27
C(13)	−0.84	−0.95	Mn(1)−C(21)	0.32	0.35
C(19)	−1.18	−1.07			

[a] Charges in electrons.

In the case of **1-HS** the NPA calculations reveal that the carbon atoms formally bonded to manganese bear appreciable negative charges. For C(1), C(2), and C(3) the small WBI values of 0.12, 0.08, and 0.16, respectively, are suggestive of predominantly ionic manganese−carbon bonding to the $[\eta^3\text{-}(Me_3Si)_2C_3H_3)_3\}]^-$ ligand in this spin state. However, the WBI values for C(11) and C(21) of 0.30 and 0.32, respectively, are indicative of polar-covalent bonding. Upon formation of **1-IS**, a significant decrease in the atomic charge on Mn(1) is observed, and in light of the increases in the WBI for the carbon atoms engaged in η^3-bonding to values in the range 0.26−0.38 it can be concluded that there is a greater covalent contribution to the manganese−carbon bonding in **1-IS**, which is fully consistent with the shorter Mn−C bond distances. It seems likely, therefore, that the increased orbital participation in the metal−ligand bonding in **1-IS** is responsible for the formation of the $S = 3/2$ spin state.

Since our work is the first theoretical investigation the manganese(II)−allyl bond, meaningful comparisons of our calculations with other manganese allyl complexes could not be undertaken. Although one other example of a manganese(II) allyl complex, the β-diketiminiate [{HC(CMeNAr)$_2$}Mn(η^1-C_3H_5)], is now known,[28] no comment on the nature of the metal−ligand bonding was made. However, there have been several reports describing experimental evidence of the ionic nature of the bonding in the related manganese cyclopentadienide complexes Cp_2Mn[29−31] and $(Me_3SiC_5H_4)_2Mn$,[32] and it would seem that these cyclopentadienide derivatives are similar in many respects to the anion **1**.

Conclusion

The calculations on the manganese(II) tris-allyl anions $[Mn\{\eta^x\text{-}(C_3H_3R_2)_3\}]^-$, where x denotes a combination of η^3- and η^1-bonded ligands and where R = Me_3Si or H, have allowed several important conclusions pertaining to the structure and bonding within compounds of this type. Of the various spin states available to the manganese(II) ion, the high-spin configuration is found in the ground state at the levels of theory applied. The mixed η^3:η^1:η^1 hapticities of the allyl ligands and

(22) Goldenburg, N. *Trans. Faraday Soc.* **1940**, *36*, 847.
(23) Chapps, G. E.; McCann, S. W.; Wickman, H. H.; Sherwood, R. C. *J. Chem. Phys.* **1974**, *60*, 990. (b) Harris, G. *J. Chem. Phys.* **1968**, *48*, 2191. (c) Scheidt, W. R.; Reed, C. A. *Chem. Rev.* **1981**, *81*, 543. (d) Birdy, R.; Behere, D. V.; Mitra, S. *J. Chem. Phys.* **1983**, *78*, 1453.
(24) Kahn, O. *Molecular Magnetism*; VCH: New York, 1993.
(25) Streitweiser, A.; Bachrach, S. M.; Dorigo, A.; von Ragué Schleyer, P. In *Lithium Chemistry: A Theoretical and Experimental Overview*; Sapse, A.-M., von Ragué Schleyer, P., Eds.; J. Wiley and Sons Inc.: New York, 1995; Chapter 1, pp 1−43.
(26) Reed, A. E.; Curtiss, L. A.; Weinhold, F. *Chem. Rev.* **1988**, *88*, 899.
(27) Wiberg, K. *Tetrahedron* **1968**, *24*, 1083.
(28) Chai, J.; Zhu, H.; Roesky, H. W.; Yang, Z.; Jancik, V.; Herbst-Irmer, R.; Schmidt, H.-G.; Noltemeyer, M. *Organometallics* **2004**, *23*, 5003.
(29) Opitz, J. *Eur. J. Mass Spectrom.* **2001**, *7*, 55.
(30) Mutoh, H.; Masuda, S. *J. Chem. Soc., Dalton Trans.* **2002**, 1875.
(31) Switzer, M. E.; Rettig, M. F. *J. Chem. Soc., Chem. Commun.* **1972**, 687.
(32) Hebendanz, N.; Köhler, F. H.; Müller, G.; Riede, J. *J. Am. Chem. Soc.* **1986**, *108*, 3281.

the asymmetry in the bonding of the η^3-allyl ligand as observed in the experimental structure of **1** are also found in the geometry-optimized structures **1-HS** and **2-HS** and are fundamental properties of this species. Furthermore, it has been shown that, despite their considerable steric requirements, the trimethylsilyl substituents play no role in determining ligand hapticity in all the complexes studied. The manganese−(η^3-allyl) bond in **1-HS** was revealed by population analyses to be predominantly ionic in character, whereas the manganese−(η^1-allyl) bonds are more accurately described as being polar-covalent. The polarity in the manganese−allyl bond, in addition to being dependent upon the hapticity of the ligand, is also dependent upon the spin configuration of manganese since an increased covalent character in the manganese−(η^3-allyl) bonds within **1-IS** was also revealed through WBI calculations. A reinvestigation of the experimental magnetic susceptibility data of [Li(thf)$_4$][**1**] produced a Curie constant that is consistent with an $S = 3/2$ spin state in the anion [**1**]$^-$, and its existence can be attributed to the increased covalent character of the manganese−(η^3-allyl) bonds as revealed by theoretical calculations on **1-IS**.

Acknowledgment. The authors gratefully acknowledge the support provided by the University of Cambridge (R.A.L., J.M.R.) and the Max-Planck Institut für Kohlenforschung (M.B.). M.B. also wishes to thank Prof. Dr. W. Thiel for continuous support.

Supporting Information Available: Illustrations of the optimized structures of **2-HS-B** and **2-HS-C** are available free of charge via the Internet at http://pubs.acs.org.

OM060295A